A Strategy for the Assembly of Multiple Porphyrin Arrays Based on the Coordination Chemistry of Ru-Centered Porphyrin Pentamers

Chi Ching Mak,[†] Nick Bampos,*[,†] Scott L. Darling,[†] Marco Montalti,[‡] Luca Prodi,[‡] and Jeremy K. M. Sanders[†]

University Chemical Laboratory, University of Cambridge, Lensfield Road, Cambridge, CB2 1EW, UK, and Dipartimento di Chimica G. Ciamician, Università degli Studi di Bologna, I-40126 Bologna, Italy

nb10013@cam.ac.uk

Received November 3, 2000

An approach which employs pentameric porphyrin arrays as building blocks toward larger porphyrin arrays is described. Two flexible, and one relatively rigid, Ru-centered porphyrin pentamers (**1**−**3**) were synthesized and fully characterized. Their potential as building blocks toward larger porphyrin arrays has been studied via their coordination chemistry using bidentate and tetradentate ligands. DABCO (diazabicyclo[2.2.2]octane) can bind two monomeric porphyrins but was found to be too small to allow the complete formation of a 10-porphyrin array. On the other hand, titration of a larger bridging dipyridyl porphyrin ligand **17** (0.5 equiv) with **1** or **2** and tetrapyridyl ligand **18** (0.25 equiv) with **3** results in the formation of the 11-porphyrin and 21-porphyrin arrays, respectively, with the 21-porphyrin array containing porphyrins in three different metalation states. Changes in the chemical shift of the inner NH protons as well as the *ortho*- and *meso*-protons of the pyridyl groups of the porphyrin ligand clearly indicate the formation of large multiple porphyrin complexes. These studies demonstrate that by use of carefully designed building blocks and suitable bridging ligands, porphyrin arrays can be constructed with a dramatic increase in size in relatively few steps. Exploiting the fact that the strength of binding of pyridyl ligands is Ru > Zn > Ni, intra- vs intermolecular competition has been used to investigate aspects of the folding of the array. The photophysical properties of **3** are also described.

Introduction

Natural light-harvesting complexes are remarkably efficient despite involving the use of hundreds of chromophores to transfer and funnel energy over long distances to the reaction center.[1] The ability to mimic natural photosynthetic processes could provide insight into solar energy conversion and storage. Owing to the size and complexity of naturally occurring light-harvesting systems, considerable efforts have recently been directed toward the design and characterization of synthetic analogues that might elucidate or mimic key mechanisms of photon capture and energy migration processes.[2] Arrays of five or more porphyrin units have been constructed either through self-assembly of porphyrins bearing molecular recognition units[3] or the synthesis of covalent porphyrin oligomers.[4] The challenging synthesis of covalently linked porphyrin systems may impose a practical limit to the formation of large porphyrin arrays. The strategy for construction of large assemblies based solely on a covalent approach would prove too difficult with nontrivial purification and the overall yields modest. Furthermore, covalent assemblies lack structural control as a result of the restrictions inherent in the bond lengths and bond angles of the connecting units. To create larger arrays, the self-assembly approach making use of molecular recognition becomes an attractive alternative to the traditional covalent strategy. Self-assembly provides efficient access to ordered arrays by spontaneous build-up based on noncovalent interactions and directed through molecular recognition events. Because of their excellent photochemical and biomimetic properties, Zn(II) or Mg(II) ions have often been used as the central metals. However, these ions under the conditions and solvents employed in this study are relatively labile with Ks for pyridine < 10^4 M^{-1}, such that the resulting self-assembled arrays are an equilibrium mixture which favors the monomers in solution at the low concentrations employed in photophysical experiments. Ru(II)-porphy-

[†] University of Cambridge.

[‡] Università degli Studi di Bologna.

(1) (a) Deisenhofer, J.; Epp, O.; Miki, K.; Huber, R.; Michel, H. *Nature* **1985**, *318*, 618. (b) Feher, G.; Allen, J. P.; Okamura, M. Y.; Rees, D. C. *Nature* **1989**, *339*, 111. (c) Mauzerall, D. C.; Greenbaum, N. L. *Biochim. Biophys. Acta* **1989**, *974*, 119. (d) Hunter, C. N.; van Grondelle, R.; Olsen, J. D. *Trends Biochem. Sci.* **1989**, *14*, 72. (e) Barber, J.; Andersson, B. *Nature* **1994**, *370*, 31. (f) McDermott, G.; Prince, S. M.; Freer, A. A.; Hawthornthwaite-Lawless, A. M.; Papiz, M. Z.; Cogdell, R. J.; Isaacs, N. W. *Nature* **1995**, *374*, 517. (g) Karrasch, S.; Bullough, P. A.; Ghosh, R. *EMBO J.* **1995**, *14*, 631. (h) Pullerits, T.; Sundström, V. *Acc. Chem. Res.* **1996**, *29*, 381.

(2) For recent reviews of porphyrin arrays, see: (a) Chen, C.-T. In *Comprehensive Supramolecular Chemistry: Coordination Polymers*; Atwood, J. L., Davies, J. E. D., Macnicol, D. D., Vögtle, F., Eds.; Pergamon Press: New York, 1996; Vol. 5, No. 4, p 91. (b) Sanders, J. K. M. In *The Porphyrin Handbook*; Kadish, K. M., Smith, K. M., Guilard, R., Eds.; Academic Press: New York, 2000; Vol. 3, Chapter 22, p 347. (c) Ward, M. D. *Chem. Soc. Rev.* **1997**, *26*, 365.

(3) (a) Anderson, S.; Anderson, H. L.; Bashall, A.; McPartlin, M.; Sanders, J. K. M. *Angew. Chem., Int. Ed. Engl.* **1995**, *34*, 1096. (b) Drain, C. M.; Russell, K. C.; Lehn, J. M. *J. Chem. Soc., Chem. Commun.* **1996**, 337. (c) Huck, W. T. S.; Rohrer, A.; Anilkumar, A. T.; Fokkens, R. H.; Nibbering, N. M. M.; van Veggel, F. C. J. M.; Reinhoudt, D. N. *New J. Chem.* **1998**, *22*, 165. (d) Drain, C. M.; Nifiatis, F.; Vasenko, A.; Batteas, J. D. *Angew. Chem., Int. Ed.* **1998**, *37*, 2344. (e) Kumar, R. K.; Goldberg, I. *Angew. Chem., Int. Ed.* . **1998**, *37*, 3027. (f) Taylor, P. N.; Anderson, H. L. *J. Am. Chem. Soc.* **1999**, *121*, 11538.

10.1021/jo001564o CCC: $20.00
Published on Web 06/01/2001

rins, however, exhibit much stronger binding even at low concentrations; this can be harnessed in the construction of supramolecular architectures.

In light of all this, self-assembly based on metal ligand interactions becomes quite attractive, as we are afforded the freedom to change metals, ligands, and coordination geometries. In the work reported here, ruthenium was identified as a suitable metal in the construction of the large assemblies, as the interaction between pyridyl ligands and ruthenium is much stronger than that with zinc or magnesium.[5]

Although noncovalent assemblies are easily prepared, they often afford imprecise structural control, while the covalent strategy provides porphyrin arrays with some structural diversity. To harness the advantages from both strategies, we set out to apply a combination of covalent and coordination chemistry to generate large porphyrin arrays. In effect, we need to initially prepare several porphyrin pentamers by conventional covalent chemistry with one Ru-porphyrin in the center. Since Ru(II)-porphyrins are stable to substitution and exhibit strong binding affinities with nitrogen-based ligands, we believe these pentamers can be used as the semilarge building blocks which can in turn self-assemble around some core or bridging ligands, generating porphyrin arrays with a dramatic increase in size. In this report we present a complete characterization of a number of covalently linked pentamers and describe the interactions of three different covalently linked pentamers with two bidentate and one tetradentate ligand. To achieve this, we exploit the fact that the strength of coordination of pyridyl groups to metals used in this study follow the series Ru $\gg$ Zn $\gg$ Ni, and show how inter- vs intramolecular competition can be controlled through flexibility of aspects of the molecular structure. Some preliminary results have been presented elsewhere.[6]

Results and Discussion

Covalent Chemistry toward Pentameric Porphyrin Arrays. In our initial strategy for preparation of a covalently linked 9-porphyrin array,[4a] two types of porphyrins with different side-chain polarity were used in order to control chromatographic mobility and ensure that the 9-porphyrin array was easily isolated from the starting materials. A second generation strategy employed Mitsunobu condensation as the key reaction and gave a 9-porphyrin array which was designed to possess greater flexibility.[7] All the porphyrin units within this 9-porphyrin array have hexyl side chains in the β-positions, while the starting porphyrin components have either polar hydroxyl or carboxyl groups. As a result, the 9-porphyrin array derived from these polar components was very nonpolar and could be separated very easily from both starting materials and any side products due to incomplete reaction.

In the present study, we began by synthesizing two flexible porphyrin pentamers (**1** and **2**, Chart 1) and one comparatively more rigid porphyrin pentamer **3** on the basis of our second strategy. Pentamers **1** and **2** are more flexible because there are in total four three-carbon saturated alkyl chains around the core Ru-porphyrin while there are four carbon−carbon triple bonds in the case of **3**. Synthetic disconnections for the component monomers are illustrated in Scheme 1. The unsymmetrical porphyrins **4** and **5** were prepared by mixed condensation of 4-*tert*-butyl- and 4-hydroxymethyl-**9** benzaldehydes with dipyrromethane **10** followed by metalation.[8] In a similar fashion, **6** was prepared in 21% overall yield from aldehyde **11** as the unsymmetrical analogue, followed by alkaline hydrolysis of the tetraester porphyrin **12**. Mitsunobu condensation[9] of Ni-**4** or Zn-**5** porphyrin with porphyrin tetraacid **6** (0.25 equiv) in THF afforded core free-base porphyrin pentamers **7** and **8** in 58 and 73% yield, respectively. Because of the formation of four ester linkages in both pentamers **7** and **8**, the ^{1}H NMR spectra exhibited a sharp singlet in the region δ 5.2−5.5 ppm corresponding to eight benzylic protons resulting from the four consecutive condensation reactions. Additional structural characterization was provided by the correct integral intensities of the *meso*-proton signals for the peripheral and core porphyrin units (4:1) and the molecular ion peaks in the MALDI spectra at *m*/*z* 5185 $(M + H)^+$ and 5212 $(M + H)^+$ for **7** and **8**, respectively, indicating complete reaction of **6** with four peripheral Ni-**4** or Zn-**5** porphyrins, respectively.

Metalation of **7** and **8** with $Ru_3(CO)_{12}$ in refluxing toluene[10] provided Ru-centered pentamers **1** and **2** as deep red solids in 66 and 61% yield, respectively. The absence of reactive functional groups on the periphery of precursors **7** and **8** eliminated Ru-mediated side reactions during metalation. Successful metalation places the Ru-coordinated CO ligand axially on one face of the porphyrin, such that the *ortho*-aromatic protons of the phenyl groups on the core porphyrin which are equivalent (doublet) for **7** and **8** before metalation, become inequiva-

(4) (a) Mak, C. C.; Bampos, N.; Sanders, J. K. M. *Angew. Chem., Int. Ed.* **1998**, *37*, 3020. (b) Davila, J.; Harriman, A.; Milgrom, L. R. *Chem. Phys. Lett.* **1987**, *136*, 427. (c) Dubowchik, G. M.; Hamilton, A. D. *J. Chem. Soc., Chem. Commun.* **1987**, 293. (d) Wennerström, O.; Ericsson, H.; Raston.; I.; Svensson, S.; Pimlott, W. *Tetrahedron Lett.* **1989**, *30*, 1129. (e) Nagata, T.; Osuka, A.; Maruyama, K. *J. Am. Chem. Soc.* **1990**, *112*, 3054. (f) Osuka, A.; Liu, B.; Maruyama, K. *Chem. Lett.* **1993**, 949. (g) Prathapan, S.; Johnson, T. E.; Lindsey, J. S. *J. Am. Chem. Soc.* **1993**, *115*, 7519. (h) Seth, J.; Palaniappan, V.; Johnson, T. E.; Prathapan, S.; Lindsey, J. S.; Bocian, D. F. *J. Am. Chem. Soc.* **1994**, *116*, 10578. (i) Wagner, R. W.; Johnson, T. E.; Lindsey, J. S. *J. Am. Chem. Soc.* **1996**, *118*, 11166. (j) Anderson, H. L.; Martin, S. J.; Bradley, D. D. C. *Angew. Chem., Int. Ed. Engl.* **1994**, *33*, 655. (k) Anderson, S.; Anderson, H. L.; Sanders, J. K. M. *J. Chem. Soc., Perkin Trans. 1* **1995**, 2247. (l) Osuka, A.; Tanabe, N.; Nakajima, S.; Maruyama, K. *J. Chem. Soc., Perkin Trans. 2* **1996**, 199. (m) Officer, D. L.; Burrell, A. K.; Reid, D. C. W. *J. Chem. Soc., Chem. Commun.* **1996**, 1657. (n) Mongin, O.; Papamicaël, C.; Hoyler, N.; Gossauer, A. *J. Org. Chem.* **1998**, *63*, 5568. (o) Vicente, M. G. H.; Cancilla, M. T.; Lebrilla, C. B.; Smith, K. M. *J. Chem. Soc., Chem. Commun.* **1998**, 2355. (p) Biemans, H. A. M.; Rowan, A. E.; Verhoeven, A.; Vanoppen, P.; Latterini, L.; Foekema, J.; Schenning, A. P. H. J.; Meijer, E. W.; de Schryver, F. C.; Nolte, R. J. M. *J. Am. Chem. Soc.* **1998**, *120*, 11054. (q) Nakano, A.; Osuka, A.; Yamazaki, I.; Yamazaki, T.; Nishimura, Y. *Angew. Chem., Int. Ed.* **1998**, *37*, 3023. (r) Li, J.; Diers, J. R.; Seth, J.; Yang, S. I.; Bocian, D. F.; Holten, D.; Lindsey, J. S. *J. Org. Chem.* **1999**, *64*, 9090. (s) Li, J.; Lindsey, J. S. *J. Org. Chem.* **1999**, *64*, 9101. (s) Aratani, N.; Osuka, A.; Kim, Y. H.; Jeong, D. H.; Kim, D *Angew. Chem., Int. Ed.* **2000**, *39*, 1458.

(5) Webb, S. J.; Sanders, J. K. M. *Inorg. Chem.* **2000**, *39*, 5912.

(6) Mak, C. C.; Bampos, N.; Sanders, J. K. M. *J. Chem. Soc., Chem. Commun.* **1999**, 1085.

(7) (a) Mak, C. C.; Pomeranc, D.; Montalti, M.; Prodi, L.; Sanders, J. K. M. *J. Chem. Soc., Chem. Commun.* **1999**, 1083. (b) Zeng, F.; Zimmerman, S. C. *J. Am. Chem. Soc.* **1996**, *118*, 5326.

(8) (a) Vidal-Ferran, A.; Bampos, N.; Sanders, J. K. M. *Inorg. Chem.* **1997**, *36*, 6117. (b) Clyde-Watson, Z.; Vidal-Ferran, A.; Twyman, L. J.; Walter, C. J.; McCallien, D. W. J.; Fanni, S.; Bampos, N.; Wylie, R. S.; Sanders, J. K. M. *New. J. Chem.* **1998**, *22*, 493. (c) Twyman, L. J.; Sanders, J. K. M. *Tetrahedron Lett.* **1999**, *40*, 6681.

(9) (a) Mitsunobu, O. *Synthesis* **1981**, 1. (b) Hughes, D. L. *Org. React.* **1992**, *42*, 335.

(10) Barley, M.; Becker, J. Y.; Domazetis, G.; Dolphin, D.; James, B. R. *Can. J. Chem.* **1983**, *61*, 2389.

Chart 1

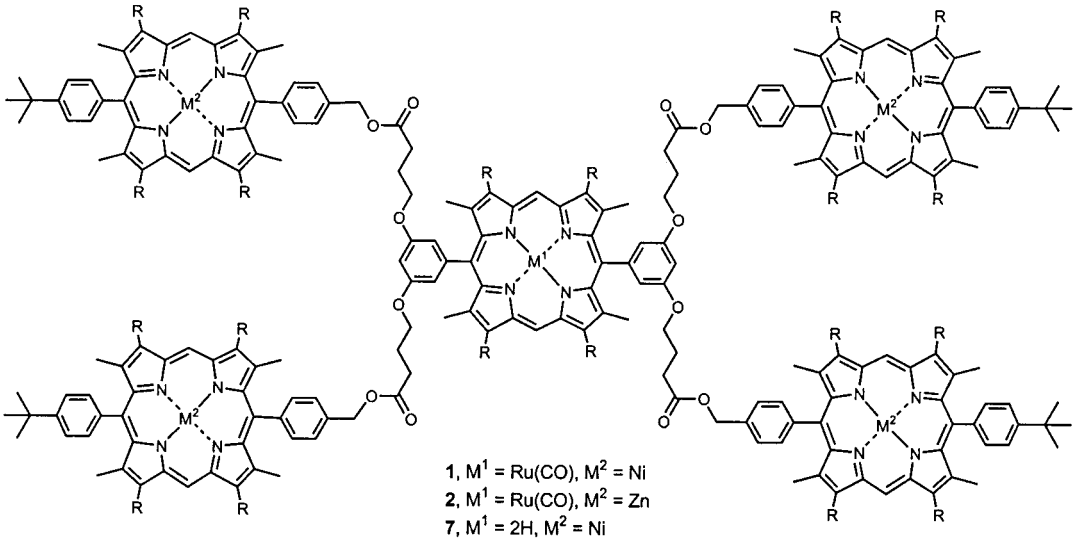

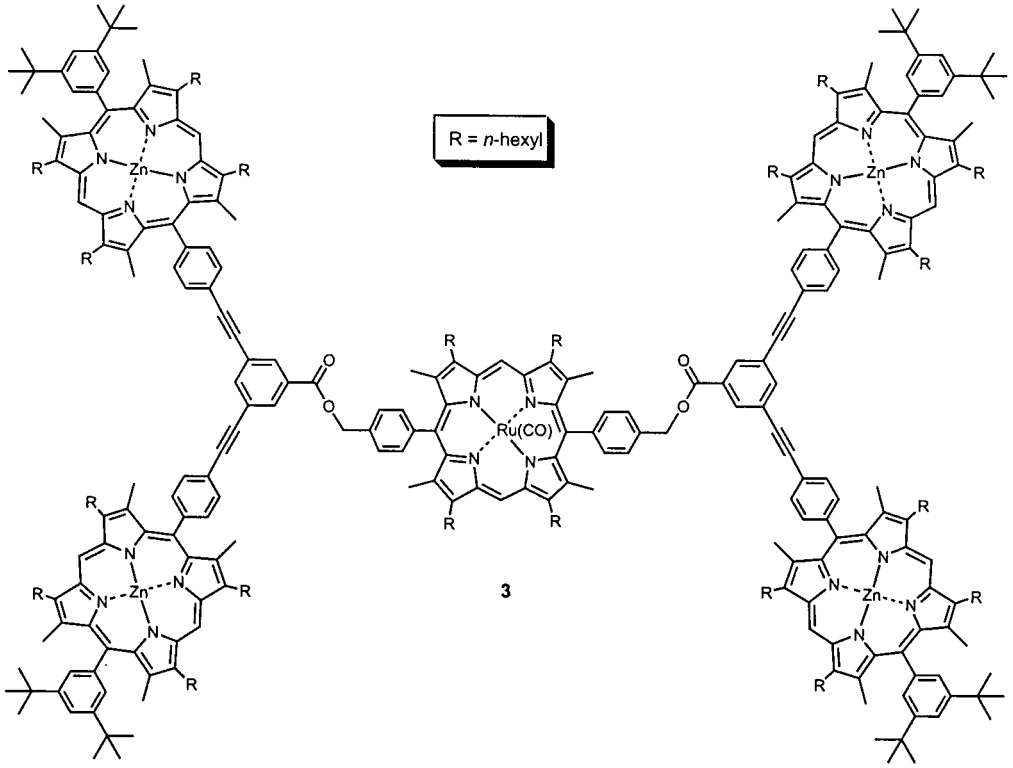

lent and give rise to two sets of signals for **1** and **2** in the δ 7.2−7.5 ppm region after metalation. Further evidence of successful metalation is offered by the disappearance of the inner NH proton signals in the ^{1}H NMR spectra and the appearance of a new molecular ion peak in the MALDI mass spectra (with loss of CO)[11] at *m*/*z* 5283 and 5314 for **1** and **2**, respectively.

For the synthesis of the rigid pentamer **3**, the functional groups on the core and peripheral units were reversed. The peripheral bis-porphyrin unit **13**, which was prepared from 3,5-diiodobenzoic acid **14**[12] and **15**[4a] (Scheme 2), now bears the carboxylic group while the core Ru-porphyrin **16** contains the hydroxyl groups. Mitsunobu condensation of **13** and **16** (0.5 equiv) afforded **3** in 21% yield. While the pyrrolic methyl signals from the core porphyrin were clearly separated from those of the peripheral porphyrins and the *ortho*-aromatic protons of the phenyl groups on the core porphyrin were inequivalent in **1** and **2**, only broad resonances corresponding to these signals were observed in the ^{1}H NMR spectrum of **3**. A MALDI-TOF spectrum afforded the ion peak at *m*/*z* 5432 [(M − 2H − CO)$^+$], and the appearance of a proton signal at δ 5.90 ppm corresponded to the formation of two ester linkages.

(11) (a) Frauenkron, M.; Berkessel, A.; Gross, J. H. *Eur. Mass. Spectrom.* **1997**, *3*, 427.

(12) **14** was prepared by reductive deamination of 4-amino-3,5-diiodobenzoic acid: Doyle, M. P.; Dellaria, J. F., Jr.; Siegfried, B.; Bishop, S. W. *J. Org. Chem.* **1977**, *42*, 3494.

Scheme 1

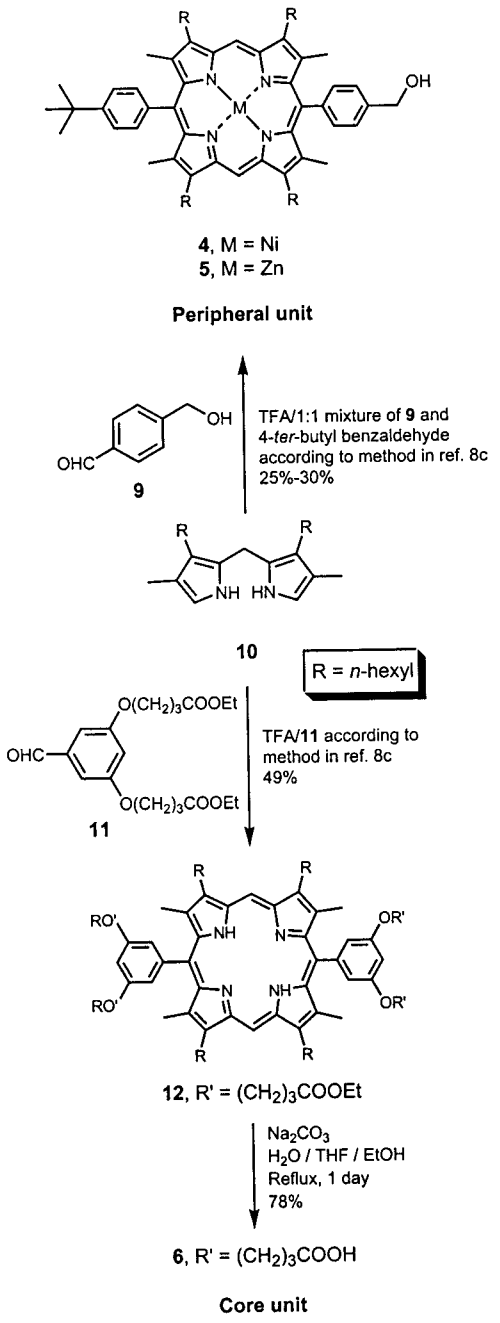

Scheme 2

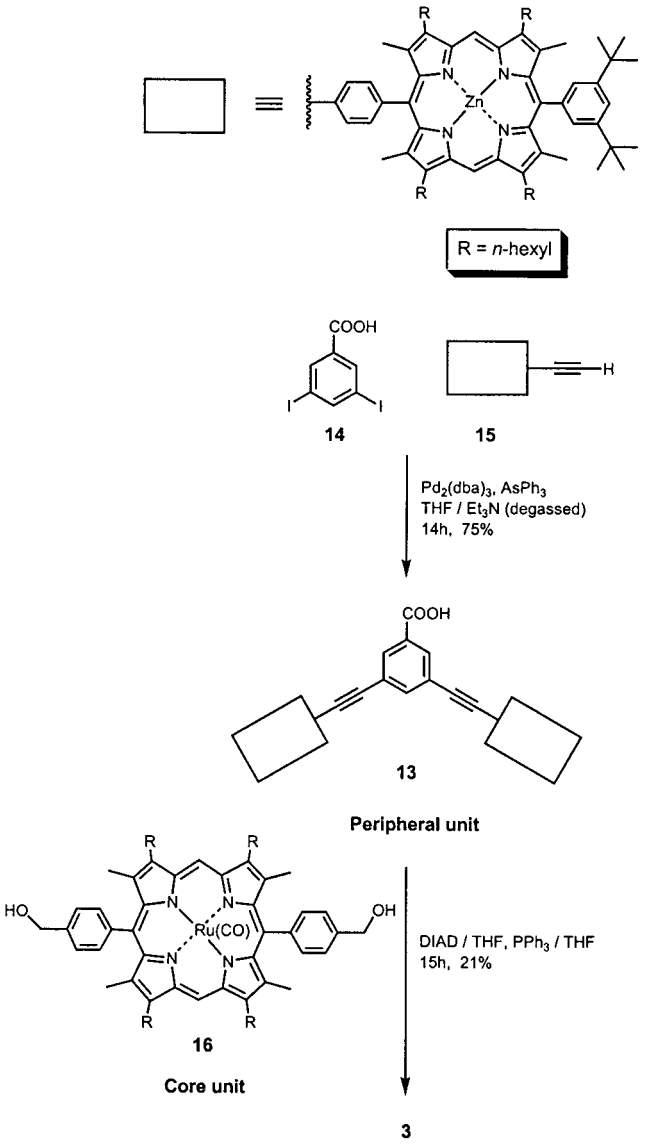

The electronic absorption spectrum of **3** in dichloromethane is essentially a superposition of the spectra of the constituent core and peripheral components (**15** with added pyridine acts as the reference compound). Photophysical studies indicate that the typical fluorescence intensity of the Zn-porphyrin component is reduced at room temperature to about 60%, in good agreement with the observed decrease of the exited state lifetime from 1.6 to 1.0 ns. From these data, a quenching rate constant of 4×10^8 s^{-1} can be calculated; an even faster rate constant, 1×10^9 s^{-1}, was found in a rigid matrix at 77 K, where the lifetime is quenched from 2.0 to 0.5 ns. According to the redox potentials and the energy of the lowest energy singlet excited state centered on the Zn-porphyrin,[13,14] S_1(Zn), in polar solvents this latter state is almost isoenergetic with a charge-separated state obtained by an electron transfer process from the Ru-porphyrin to a peripheral component. It seems unlikely that such an electron transfer process can occur in a nonpolar solvent or even in a rigid matrix at 77 K, where the charge-separated state is strongly destabilized.[14,15] As previously found for similar assemblies,[15] the most likely explanation for this phenomenon is the heavy-atom effect caused by the presence of the ruthenium centers enhancing intersystem crossing in the Zn-porphyrin units. However, the thermodynamically feasible energy transfer process to the lowest energy triplet excited state centered on the Ru-porphyrin, T_1(Ru), which lies below the S_1(Zn) state, cannot be ruled out (Figure 1). In turn, T_1(Ru) is also completely quenched, both in deaerated solution at room temperature and at 77 K in rigid matrix. Since electron transfer from T_1(Ru), which has a lower energy content than S_1(Zn), is even more disfavored, this quenching process can only be explained by an energy transfer process occurring between the two different

(13) Kalyanasundaram, K. *Photochemistry of Polypyridine and Porphyrin Complexes*; Academic Press: London, 1991.

(14) Gaines, G. L., III; O'Neil, M. P.; Svec, W. A.; Niemczyk, M. P.; Wasielewski, M. R. *J. Am. Chem. Soc.* **1990**, *113*, 719.

(15) Prodi, A.; Indelli, M. T.; Kleverlaan, C. J.; Scandola, F.; Alessio, E.; Gianferrara, T.; Marzilli, L. G. *Chem. Eur. J.* **1999**, *5*, 2668.

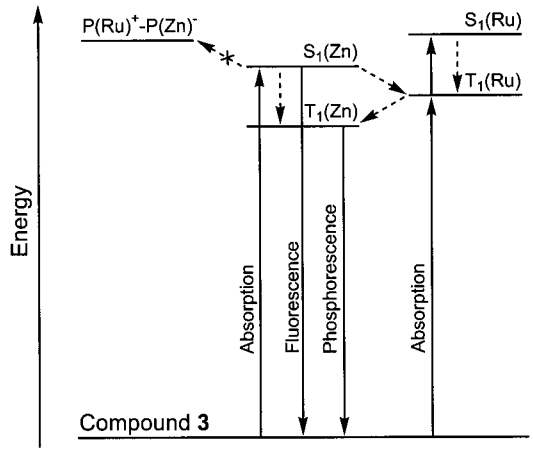

Figure 1. Energy diagram for the transitions of **3**.

kinds of component, this time from T_1(Ru), centered on the core unit, to T_1(Zn), localized on the periphery. The T_1(Zn) is in turn luminescent at 77 K, giving the typical phosphorescence band with $\lambda_{max} = 720$ nm and lifetime of 60 ms (at 77 K).

Coordination Chemistry of the Pentameric Porphyrin Arrays. Ru-porphyrin monomers have been used as building blocks for small porphyrin arrays,[16] but there is little literature precedent for using larger porphyrin building blocks to self-assemble around a multidentate ligand to achieve large porphyrin arrays. Our first aim was to study the coordination properties of our three Ru-centered pentamers (**1**, **2**, and **3**), initially with bidentate ligands (DABCO or bipyridyl porphyrin **17**)[17] and then a tetradentate ligand such as tetrapyridyl porphyrin **18** (Chart 2). The progress of the coordination assembly as well as the final structure of the coordinated arrays was monitored as NMR titration experiments, typically on 3−8 mM solutions.

(a) Titration with DABCO. The coordination properties of the central Ru-porphyrin of **1** and **2** are modulated by the Ni/Zn chemistry of the peripheral porphyrins in addition to the spatial constraints imparted on the complexes by the "sweep" of the flexible peripheral Ni/Zn-porphyrins. The ^{1}H NMR shifts of DABCO-bound Ru and/or Zn are diagnostic of the coordinating environment by virtue of the porphyrin ring currents (Figure 2). In-plane Ru draws a coordinated nitrogen atom closer to the shielding region of the porphyrin plane than does a pyramidal Zn analogue, and the greater deshielding is reflected in a high-field shift of the meso resonance. Titration experiments on the respective core free-base pentamers **7** and **8** (differing only in the metal at the peripheral sites) were performed as control experiments. Since Ni-porphyrins exhibit a low affinity for nitrogenous ligands (for piperidine, $K \approx 200$ M^{-1} in toluene at 22 °C),[18] no change was observed in the ^{1}H NMR spectra when up to 1.5 equiv of DABCO was added to **7**. On the other hand, significant changes were observed during the titration with **8** (Figure 3). Most notably, a new upfield signal at around δ −5.0 ppm was observed when less than 2 equiv of DABCO was added (Figures 3b and 3c). This upfield signal, which is diagnostic of the ligand sandwiched between two Zn-porphyrins,[4a,19] disappeared after addition of more than 2 equiv of DABCO (Figure 3d) as there are only two intramolecular binding sites within **8**—excess DABCO will be in fast exchange.

Titration of DABCO into a mM solution of **1** gave spectra which clearly indicated formation of both mono-ligated and bis-ligated porphyrin complexes when up to 0.5 equiv of DABCO was added (Figure 4). The ^{1}H NMR and NOESY spectra suggested that these two species were in slow exchange on the chemical shift time scale but fast on the T_1 time scale, giving a sharp signal at −5.68 ppm (bis-ligated complex) and two triplet resonances at 0.62 and −3.65 ppm (mono-ligated complex). Methylene protons of DABCO which are closer to the Ru center in the mononuclear complex will experience a stronger ring current effect and display an upfield triplet resonance (−3.65 ppm). This equilibrium may be attributed to the small size of DABCO, such that the steric interaction between the peripheral porphyrins of the two pentamers does not favor the formation of a 10-porphyrin array.

When less than 0.5 equiv of DABCO was added to **2** (Figure 5), the signals observed previously in the case of **1** were absent. Instead, two new triplets were recorded at −5.20 and −5.58 ppm as a result of the *intra*molecular coordination of DABCO between one peripheral Zn-porphyrin and the core Ru-porphyrin (Figure 5a). As the Ru-porphyrin has a stronger binding affinity than that of Zn component, the methylene protons of the ligand closer to the Ru center (−5.58 ppm) exhibited a sharper upfield triplet signal. Intramolecular coordination is favored over the intermolecular construction of the 10-porphyrin array by the flexible linkers between the core and the 4 peripheral porphyrins. In the presence of 2 equiv of DABCO, an additional signal, which is assigned to the ligand sandwiched intramolecularly between two Zn-porphyrins (observed previously in **8**), appears (Figure 5d).

DABCO cannot form an analogous intramolecular complex between the Ru- and Zn-porphyrins in **3**, due to the rigid linkers. Instead, a sharp signal at −5.72 ppm attributed to the formation of the 10-porphyrin array was observed when less than 0.5 equiv of ligand was added (Figures 6a and 6b). Increasing the amount of DABCO to 1 or 2 equiv (Figures 6c and 6d) results in broad resonances in the range −4.5 to −5.7 ppm. This phenomenon may be due to an equilibrium mixture of complexes, in which DABCO is *intermolecularly* bound between two Ru-porphyrins, two Zn-porphyrins, or one Ru- and one Zn-porphyrin (Figure 7). The evidence therefore suggests that DABCO is too small a bridging ligand for the clean formation of 10-porphyrin arrays on the basis of the Ru-centered pentamers prepared in this

(16) For Ru-porphyrin monomers used as building blocks in porphyrin arrays, see: (a) Anderson, H. L.; Hunter, C. A.; Sanders, J. K. M. *J. Chem. Soc., Chem. Commun.* **1989**, 226. (b) Alessio, E.; Macchi, M.; Heath, S.; Marzilli, L. G. *J. Chem. Soc., Chem. Commun.* **1996**, 1411. (c) Funatsu, K.; Kimura, A.; Imamura, T.; Ichimura, A.; Sasaki, Y. *Inorg. Chem.* **1997**, *36*, 1625. (d) Funatsu, K.; Imamura, T.; Ichimura, A.; Sasaki, Y. *Inorg. Chem.* **1998**, *37*, 1798. (e) Funatsu, K.; Imamura, T.; Ichimura, A.; Sasaki, Y. *Inorg. Chem.* **1998**, *37*, 4986.

(17) Kim, H.-J.; Bampos, N.; Sanders, J. K. M. *J. Am. Chem. Soc.* **1999**, *121*, 8120.

(18) (a) LaMar, G. N.; Walker, F. A. In *The Porphyrins*; Dolphin, D., Ed.; Academic Press: New York, 1979; Vol. IV, pp 129−130. (b) Walker, F. A.; Hui, E.; Walker, J. M. *J. Am. Chem. Soc.* **1975**, *97*, 2390.

(19) Hunter, C. A.; Meah, M. N.; Sanders, J. K. M. *J. Am. Chem. Soc.* **1990**, *112*, 5773.

Chart 2

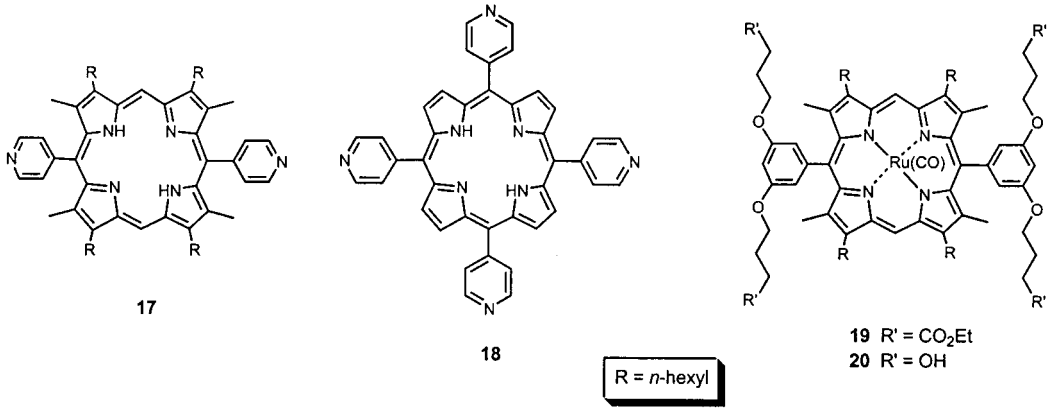

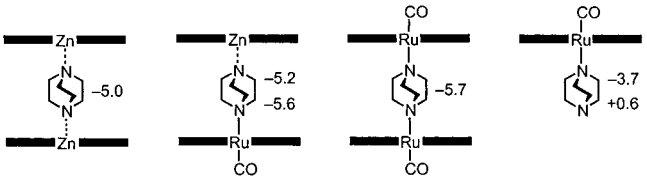

Figure 2. Chemical shifts (δ ppm) of the Ru- and/or Zn-bound DABCO ligand in the ^{1}H NMR spectrum. For comparison, free DABCO appears at 2.7 ppm.

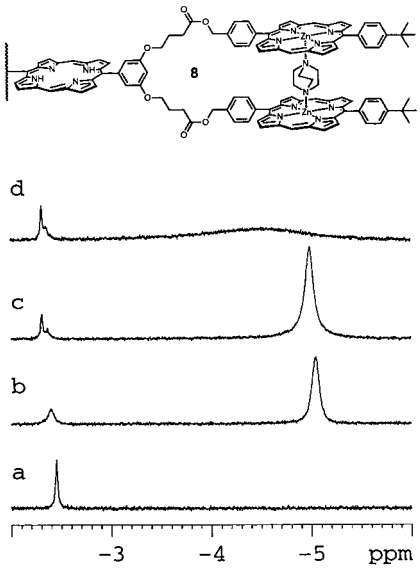

Figure 3. High-field region of the ^{1}H NMR spectrum of **8** (500 MHz, $CDCl_3$, 300 K), showing the appearance of the bound ligand resonance as a function of the number of equiv of DABCO added: (a) 0, (b) 1.0, (c) 2.0, (d) 2.5. The structure above represents only half of the **8**·DABCO complex.

study, although the titration of DABCO with **3** may provide the 10-porphyrin array over a narrow stoichiometric regime.

(b) Titration with Dipyridyl Porphyrin 17. The large size of ligand **17** would be expected to prevent intramolecular coordination between either two Zn-porphyrins or between one Ru- and one Zn-porphyrin in the manner discussed above and should also relieve steric interactions between two bound pentamers. Indeed, titration of **1** or **2** with less than 0.5 equiv of dipyridyl porphyrin **17** clearly indicated the intermolecular assembly of the flexible pentamers around the dipyridyl ligand, forming an 11-porphyrin array in both cases. The

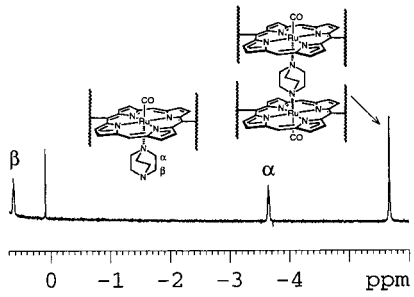

Figure 4. High-field region of the ^{1}H NMR spectrum of **1** (500 MHz, $CDCl_3$, 300 K), showing the appearance of the bound ligand resonances upon addition of 0.5 equiv of DABCO. This region of the spectrum was free of resonances in the absence of added ligand.

chemical shifts for *ortho*- and *meta*-protons of the pyridyl groups of the porphyrin ligand (significant shift to lower δ values) were diagnostic of the coordination to the axial position of the central Ru metal of the porphyrin pentamers. In addition, the changes in chemical shift of the inner NH and *meso*-H on complexation clearly reflect the effect of the porphyrin ring current.

Compared to the corresponding chemical shifts of the free ligand, significant upfield shifts were observed for all the proton resonances mentioned previously (Figure 8a–c). Furthermore, the integral intensity ratios of the signals of the porphyrin pentamers and of NH or *meso*-H of the bridging ligand **17** confirmed the integrity of the porphyrin arrays. Titration of Ru-porphyrin monomer **19** with **17** (0.5 equiv) gave slightly upfield shifted signals for all of the inner NH, *meso*-H, and 2,6-pyridyl protons of **17** (Figure 8d).

(c) Titration with Tetrapyridyl Porphyrin 18. The coordination of **18** to four Ru-porphyrin monomers has been reported.[16d] However, owing to the large size of our pentamers, the possibility of tetrapyridyl porphyrin **18** coordinating less than four pentamers cannot be excluded even when 4 equiv of a pentamer has been added. As the ring current effect around **18** is cumulatively dependent on the number of bound Ru-porphyrins,[16d] titration of **18** with less than 4 equiv of Ru-porphyrin monomer **19** should produce a statistical mixture of complexes. Each complex will give rise to different inner NH-proton signals, the chemical shift of which will be sensitive to the number of Ru-porphyrin around ligand **18**.[20]

(20) Kariya, N.; Imamura, T.; Sasaki, Y. *Inorg. Chem.* **1997**, *36*, 833.

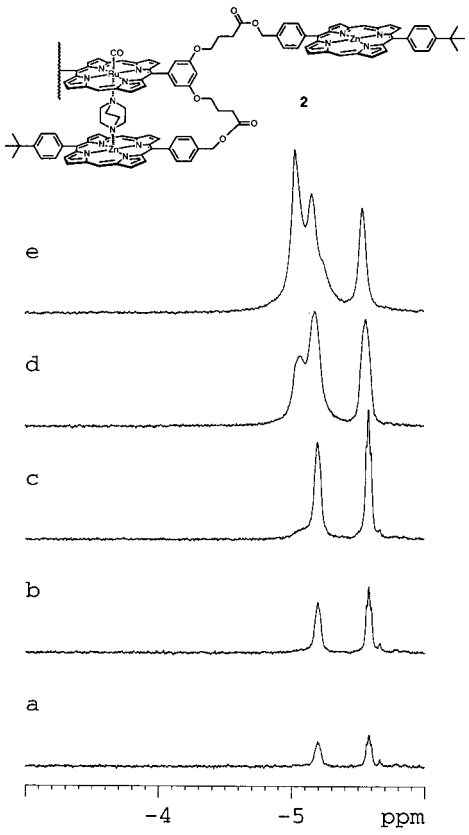

Figure 5. High-field region of the ^{1}H NMR spectrum of **2** (500 MHz, $CDCl_3$, 300 K), showing the appearance of the bound ligand resonances as a function of the number of equiv of DABCO added: (a) 0.25, (b) 0.5, (c) 1.0, (d) 2.0, (e) 3.0. This region of the spectrum was free of resonances in the absence of added ligand. The structure above shows a DABCO molecule coordinating to the central Ru-porphyrin of **2** and one of the peripheral Zn-porphyrins; only half the molecule is represented.

Four types of NH proton signals corresponding to the binding of one to four Ru-porphyrins were observed when 2 equiv of Ru-porphyrin monomer **20** was added to tetrapyridyl porphyrin **18** (Figure 9). The value of the chemical shift for the NH signals appears incrementally upfield (by δ 0.5 ppm) with each additional bound Ru-porphyrin. With these results in hand, we were able to perform titration experiments of various pentamers with **18** (Figure 10) and follow the progress of the reaction by registering the upfield shift of the NH proton signals. Addition of 4 equiv of flexible pentamer **1** to **18** (Figure 10b) led to coordination of a maximum of 3 equiv of **1**, resulting in a 16-porphyrin array. The shape of the resulting complex, with the four flexible terminal Ni porphyrins of the constituent pentamer **1** sweeping a large volume in space, may account for this result. Addition of Ru-porphyrin monomer **20** to this mixture caused scrambling (Figure 10c) as the smaller porphyrin displaced the pentamers in the complex, giving a non-statistical mixture of complexes including both three- and four-coordinated species. On the other hand, titration with 4 equiv of the rigid pentamer **3** indicated coordination of 4 equiv of **3**, yielding a 21-porphyrin array (Figure 10d). The rigid structure of the pentamer **3** offers efficient "spatial" coordination around the core ligand **18**, compared to the flexible pentamer **1**, thus favoring the saturated 21-porphyrin complex. A reduced upfield shift

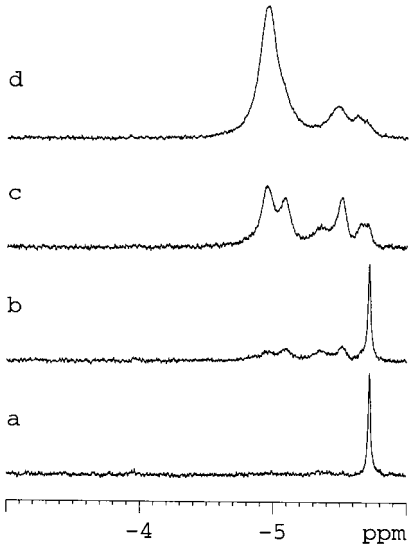

Figure 6. High-field region of the ^{1}H NMR spectrum of **3** (500 MHz, $CDCl_3$, 300 K), showing the appearance of the bound ligand resonances as a function of the number of equiv of DABCO added: (a) 0.25, (b) 0.5, (c) 1.0, (d) 2.0. This region of the spectrum was free of resonances in the absence of added ligand.

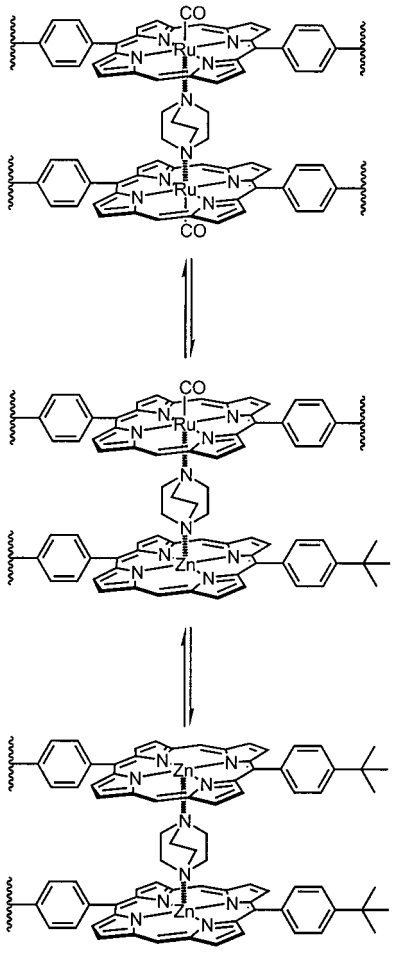

Figure 7. Possible equilibria for DABCO sandwiched intermolecularly between two molecules of rigid pentamer **3** involving the core Ru and peripheral Zn porphyrins.

was detected for the NH-proton signals of both the three- and four-coordinated complexes describe above, possibly

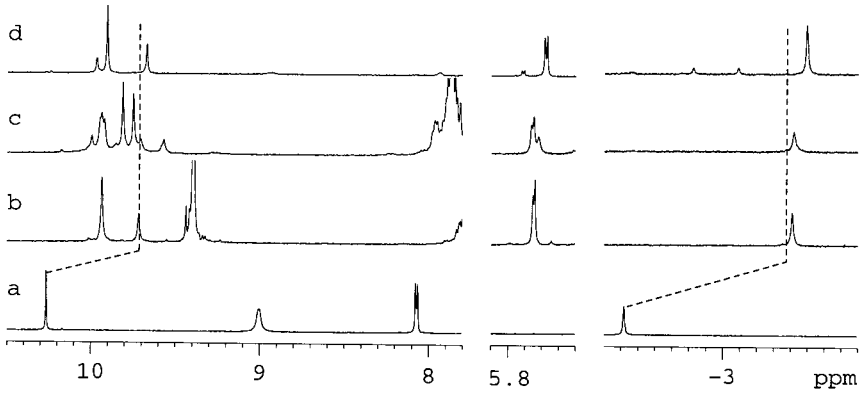

Figure 8. Selected regions of the ^{1}H NMR spectrum (500 MHz, $CDCl_3$, 300 K) showing (left to right) the *meso*, 3,5-pyridyl, and inner NH proton resonances of **17**: (a) free ligand, (b) with 2 equiv of pentamer **1**, (c) with 2 equiv of pentamer **2**, (d) with 2 equiv of monomer **19**.

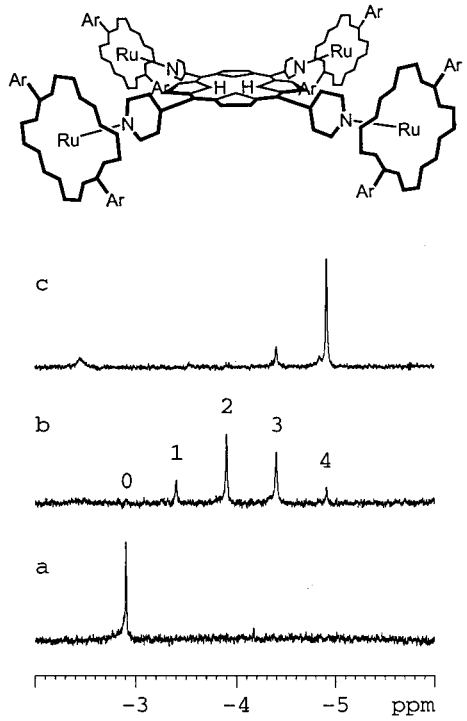

Figure 9. High-field region of the ^{1}H NMR spectrum of **18** (500 MHz, $CDCl_3$, 300 K) showing the inner NH protons resonances (a) free ligand, (b) with 2 equiv of Ru monomer **20**, (c) with 4 equiv of Ru monomer **20**. The structure above represents four Ru-porphyrins bound to **18**.

attributed to the smaller cumulative shielding effect of the pentamers due to some steric interactions around the tetrapyridyl porphyrin **18**, compared to case described for the monomer **20**.

Conclusions

This paper reports the synthesis and characterization of new Ru-centered pentameric porphyrin arrays. Judicious use of functional groups at the porphyrin periphery help separate the desired material from the starting material and possible side products. The NMR titration experiments demonstrate the potential for these porphyrin arrays as large building blocks, self-assembling around bi- and tetraddentate ligands to provide even larger porphyrin arrays, by exploiting the inherent

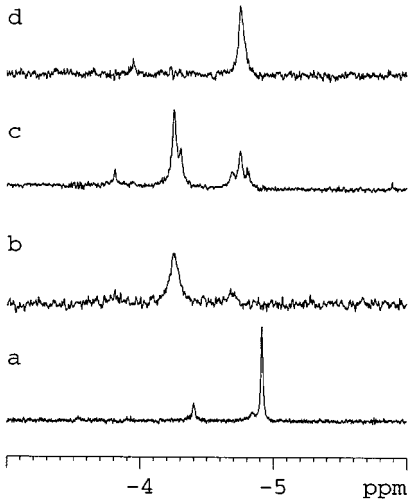

Figure 10. High-field region of the ^{1}H NMR spectrum of **18** (500 MHz, $CDCl_3$, 300 K) showing the inner NH protons resonances: (a) with 4 equiv of monomer **20**, (b) with 4 equiv of pentamer **1**, (c) with 4 equiv of pentamer **1** and trace amount of monomer **13**, (d) with 4 equiv of pentamer **3**.

flexibility of the molecules prepared and the binding affinity of pyridyl ligands to three metals in the order Ru > Zn > Ni. The steric effect due to the porphyrin arrays surrounding the core or bridging ligands is the crucial factor controlling the formation of the large porphyrin complexes. By careful design of building blocks and choosing suitable bridging ligands, porphyrin arrays can be fabricated with the size increasing dramatically with very few steps. Photolytic removal and substitution of the CO by additional ligands expands the scope of this approach even further.[21] While the present choice of metals and the inclusion of amines is not ideal for photochemical studies, we aim to exploit and extend the methodology described here to design large arrays with more suitable metals and functional groups.

Experimental Section

^{1}H NMR spectra (250, 400, or 500 MHz) were recorded on Bruker AC-250, AM-400, or DRX-500 spectrometers, respectively. ^{13}C NMR spectra were obtained on an AM-400 operating at 100.6 MHz or a Bruker AC-250 operating at 62.9 MHz. All

(21) Darling, S. L.; Mak, C. C.; Bampos, N.; Feeder, N.; Teat, S. J.; Sanders, J. K. M. *New J. Chem.* **1999**, *23*, 359.

NMR measurements were carried out at room temperature in deuteriochloroform unless otherwise specified. Routine UV/visible spectra were obtained on a Uvikon 810 spectrometer in 10 mm oven-dried cuvettes. Distilled solvents were used throughout and when used dry were freshly obtained from solvent stills. Triethylamine and dichloromethane (CH_2Cl_2) were distilled from CaH_2 under argon while toluene and tetrahydrofuran (THF) were distilled from CaH_2 or sodium, also under argon. Free-base porphyrins were converted into zinc/nickel complexes in near quantitative yield by treatment with zinc/nickel acetate dihydrate in CH_2Cl_2 or refluxing chloroform, respectively. MALDI-TOF mass spectra were recorded on a Kratos Analytical Ltd, Kompact MALDI IV mass spectrometer. A nitrogen laser (337 nm, 85 kW peak laser power, 3 ns pulse width) was used to desorb the sample ions, and the instrument was operated in linear time-of-flight mode with an accelerating potential of 20 kV. Results from 50 laser shots were signal averaged to give one spectrum. An aliquot (1 μL) of a saturated solution of the matrix (sinapinic acid) was deposited on the sample plate surface. Before the matrix completely dried, a small volume (1 μL) of analytes (dissolved in dichloromethane/chloroform at 1 mg/mL) was layered on the top of the matrix and allowed to air-dry.

Absorption spectra were recorded with a Perkin-Elmer λ 16 spectrophotometer. Uncorrected emission spectra, corrected excitation spectra, and phosphorescence lifetimes were obtained with a Perkin-Elmer LS50 spectrofluorimeter. The fluorescence lifetimes (uncertainty, ±5%) were obtained with an Edinburgh single-photon counting apparatus (D_2 filled flash lamp). Emission spectra in a CH_2Cl_2 rigid matrix at 77 K were recorded using quartz tubes immersed in a quartz Dewar filled with liquid nitrogen. To allow comparison of emission intensities, corrections for instrumental response, inner filter effects, and phototube sensitivity were performed.[22]

Dipyrrole **10**[8c] and porphyrins **15**[4a] and **17**[17] were prepared according to previously published procedures. Tetrapyridyl porphyrin **18** was used as purchased from Aldrich. **19** and **20** are the metalated analogues[6] of **12** and its tetraacid[7] prepared according to the method described for **1** and **2** below.

4-Hydroxymethylbenzaldehyde (9).[23] A solution of terephthalaldehyde (15.0 g, 112 mmol) in THF (100 mL) was cooled to 0 °C. Sodium borohydride (1.50 g, 39.5 mmol) was added in one portion at the same temperature and the mixture stirred at room temperature for 1 h. Solvent was removed and the residue taken up in EtOAc (200 mL). The solution was then washed with water (2 × 100 mL) and brine and dried (anhydrous $MgSO_4$). Upon removal of the solvent, the residue was chromatographed on SiO_2, eluting with hexane/ethyl acetate (gradient 2:1 to 1:1) to give **9** as a white solid (9.5 g, 62%): ^{1}H NMR (250 MHz, $CDCl_3$) δ 4.80 (s, 2 H, CH_2OH), 7.53 (d, J = 8.0 Hz, 2 H, ArH), 7.87 (d, J = 8.0 Hz, 2 H, ArH), 10.0 (s, 1 H, CHO); ^{13}C NMR (62.9 MHz, $CDCl_3$) δ 64.4, 126.9, 130.0, 135.5, 148.1, 192.3.

3,5-Bis(ethoxycarbonylethylpropyloxy)benzaldehyde (11). A solution of 3,5-dihydroxybenzaldehyde (1.0 g, 7.2 mmol) and K_2CO_3 (4.2 g, 30.4 mmol) in DMF (50 mL) was heated to 80 °C under argon for 1 h. 4-Bromoethylbutanoate (3.5 g 18.0 mmol) was added and the reaction mixture stirred for 1 d at 80 °C. EtOAc (100 mL) was added and the reaction mixture washed with water (3 × 100 mL), after which the organic layer was separated, washed with brine (100 mL), and dried ($MgSO_4$) and the solvent removed. The resulting crude product was purified by SiO_2 chromatography eluting with hexane/ethyl acetate (gradient 4:1 to 3:1) to give **11** as a white solid (2.5 g, 94%): ^{1}H NMR (250 MHz, $CDCl_3$) δ 1.26 (t, J = 7.1 Hz, 6 H, COOCH$_2$CH_3), 2.11 (tt, J = 6.1 and 7.2 Hz, 4 H, OCH$_2$CH_2CH$_2$), 2.50 (t, J = 7.2 Hz, 4 H, OCH$_2$CH$_2$CH_2), 4.03 (t, J = 6.1 Hz, 4 H, OCH_2CH$_2$CH$_2$), 4.15 (q, J = 7.1 Hz, 4 H, COOCH_2CH$_3$), 6.67 (t, J = 2.3 Hz, 1 H, ArH), 6.97 (d, J = 2.3 Hz, 2 H, ArH), 9.87 (s, 1 H, CHO); ^{13}C NMR (62.9 MHz, $CDCl_3$) δ 14.2, 24.5, 30.7, 60.5, 67.2, 107.8, 108.0, 138.4, 160.5, 173.0, 191.8; MS (FAB, m/z) 367 [(M + H)$^+$]. Anal. Calcd for $C_{19}H_{26}O_7$: C, 62.28; H, 7.15. Found: C, 61.94; H, 7.20.

5,15-Bis(3,5-(ethoxycarbonylethylpropyloxy)phenyl)-2,8,12,18-tetra(*n*-hexyl)-3,7,13,17-tetramethylporphyrin (12). 12 was obtained as a red powder in 49% overall yield from **10** and **11** according to a previously published procedure:[8] ^{1}H NMR (250 MHz, $CDCl_3$) δ −2.43 (s, 2 H, NH), 0.92 (t, J = 7.1 Hz, 12 H, (CH$_2$)$_5$CH_3), 1.25 (t, J = 7.1 Hz, 12 H, COOCH$_2$CH_3), 1.32−1.57 (2 × m, 16 H, (CH$_2$)$_3$(CH_2)$_2$CH$_3$), 1.77 (apparent quintet, J = 7.1 Hz, 8 Hz, (CH$_2$)$_2$CH_2(CH$_2$)$_2$CH$_3$), 2.18−2.25 (2 × m, 16 H, CH$_2$CH_2(CH$_2$)$_3$CH$_3$ and OCH$_2$CH_2-CH$_2$), 2.58 (t, J = 7.2 Hz, 8 H, CH_2COOEt), 2.68 (s, 12 H, pyrrolic CH_3), 3.98−4.04 (m, 8H, CH_2(CH$_2$)$_4$CH$_3$), 4.10−4.19 (2 × m, 16 H, COOCH_2CH$_3$ and OCH_2), 6.91 (t, J = 2.2 Hz, 2 H, ArH), 7.26 (d, J = 2.2 Hz, 4 H, ArH), 10.25 (s, 2 H, *meso*-H); ^{13}C NMR (62.9 MHz, $CDCl_3$) δ 14.1, 14.4, 22.8, 24.8, 26.8, 30.0, 30.9, 32.0, 33.3, 60.4, 67.3, 96.9, 102.0, 112.9, 117.6, 136.1, 141.4, 143.3, 143.9, 144.8, 159.4, 173.2; MS (FAB, m/z) 1377 [(M + 2H)$^+$]; UV/vis (CH_2Cl_2) λ_{max} (log ϵ) = 408 (5.32), 506 (4.26), 538 (3.82), 576 (3.90), 622 (3.46). Anal. Calcd for $C_{84}H_{118}N_4O_{12}$: C, 73.33; H, 8.14; N, 4.07. Found: C, 73.23; H, 8.51; N, 4.09.

5,15-Bis(3,5-(4-ether-butanoic acid)phenyl)-2,8,12,18-tetra(*n*-hexyl)-3,7,13,17-tetramethylporphyrin (6). A solution containing **12** (200 mg, 0.145 mmol) and Na_2CO_3 (200 mg, 1.89 mmol) in a mixture of water/THF/ethanol (100 mL, 1/1/2) was refluxed at 100 °C for 1 d. After removel most of the solvents, EtOAc (200 mL) was added and the solution was washed with water until the organic layer changed from green to red color. The organic layer was then separated, washed with brine, and dried ($MgSO_4$) and the solvent removed. The resulting solid was recrystallized from methanol to give **6** as a dark violet crystalline solid (142 mg, 78%): ^{1}H NMR (250 MHz, DMSO-d_6) δ −2.62 (s, 2 H, NH), 0.86 (t, J = 7.2 Hz, 12 H, (CH$_2$)$_5$CH_3), 1.25−1.55 (2 × m, 16 H, (CH$_2$)$_3$(CH_2)$_2$CH$_3$), 1.70 (apparent quintet, J = 7.2, 8 H, (CH$_2$)$_2$CH_2(CH$_2$)$_2$CH$_3$), 1.90−2.20 (2 × m, 16 H, CH$_2$CH_2(CH$_2$)$_3$CH$_3$ and OCH$_2$CH_2CH$_2$), 2.41 (t, J = 7.3 Hz, 8 H, CH_2COOH), 2.62 (s, 12 H, CH_3), 3.80−4.20 (m, 8 H, CH_2(CH$_2$)$_4$CH$_3$), 4.15 (t, J = 6.4 Hz, 8 H, OCH_2), 7.00 (t, J = 2.1 Hz, 2 H, ArH), 7.21 (d, J = 2.1 Hz, 4 H, ArH), 10.18 (s, 2 H, *meso*-H), 12.12 (s, 4 H, COOH); ^{13}C NMR (62.9 MHz, DMSO-d_6) δ 14.3, 22.6, 24.8, 26.4, 29.9, 30.6, 31.8, 33.4, 67.6, 96.8, 102.4, 112.8, 118.2, 136.5, 141.0, 143.3, 143.7, 144.7, 159.6, 174.5; UV/vis (THF) λ_{max} (log ϵ) = 408 (5.44), 504 (4.77), 580 (4.69), 538 (4.64), 610 (4.55). Anal. Calcd for $C_{76}H_{102}N_4O_{12}$: C, 72.23; H, 8.13; N, 4.43. Found: C, 71.99; H, 7.98; N, 4.06.

3,5-Diiodobenzoic Acid (14).[24] 4-Amino-3,5-diiodobenzoic acid (1.0 g, 2.6 mmol) suspended in DMF (10 mL) was added dropwise to a rapidly stirred solution of *tert*-butylnitrite and anhydrous DMF (5 mL) heated at 50 °C in a 100 mL three-necked round-bottomed flask equipped with a reflux condenser. Gas evolution was registered throughout the addition. After addition was complete, the reaction mixture was stirred for a further 15 min and then cooled to room temperature. The resulting burnt orange solution was diluted with ether (30 mL) and then poured into dilute HCl (50 mL, 3 N). After separation, the etheral solution was washed with additional dilute HCl (50 mL) and water and dried over anhydrous Na_2SO_4. Removal of ether and recrystallization from MeOH afforded **14** as a pale brown solid (0.6 g, 62%): ^{1}H NMR (250 MHz, $CDCl_3$) δ 8.29 (t, J = 1.6 Hz, 1 H, ArH), 8.39 (d, J = 1.6 Hz, 2 H, ArH); ^{13}C NMR (62.9 MHz, $CDCl_3$) δ 94.5, 138.3, 150.1, 167.4, 208.5; MS (FAB, m/z) 374 (M$^+$). Anal. Calcd for $C_7H_4I_2O_2$: C, 22.49; H, 1.08. Found: C, 22.66; H, 1.06.

Bis(Zn-porphyrin) Benzoic Acid 13. A solution containing **15** (500 mg, 0.24 mmol) **14** (85 mg, 0.11 mmol), $Pd_2(dba)_3$ (22 mg, 0.022 mmol), and $AsPh_3$ (37 mg, 0.12 mmol) in THF/Et_3N (20 mL, 1:1) in a Schlenk tube was degassed by two freeze−pump−thaw cycles. The mixture was then stirred at room temperature under argon for 14 h and the solvent

(22) Credi, A.; Prodi, L. *Spectrochim. Acta, Part A* **1998**, *54*, 159.

(23) Gennari, C.; Ceccarelli, S.; Piarulli, U.; Aboutayab, K.; Donghi, M.; Paterson, I. *Tetrahedron* **1998**, *54*, 14999.

(24) (a) Wheeler, H. L.; Liddle, L. M. *Am. Chem. J.* **1909**, *42*, 441. (b) Lulinski, P.; Skulski, L. *Bull. Chem. Soc. Jpn.* **1997**, *70*, 1665.

removed, after which the residue was extracted into EtOAc (50 mL), washed with water (2 × 50 mL) and brine, and dried. After removel of the solvent, the crude product was purified by SiO_2 chromatography eluting with hexane/ethyl acetate (gradient 1:9 to MeOH/ethyl acetate, 1:20) to give **13** as a purple solid (380 mg, 75%): ^{1}H NMR (250 MHz, $CDCl_3$) δ 0.93 (t, J = 7.0 Hz, 24 H, $(CH_2)_5CH_3$), 1.20−1.90 (3 × m, 48 H, $(CH_2)_2(CH_2)_3CH_3$), 1.53 (s, 36 H, *t-Bu*), 2.10−2.30 (m, 16 H, $CH_2CH_2(CH_2)_3CH_3$), 2.46 (s, 12 H, pyrrolic CH_3), 2.58 (s, 12 H, pyrrolic CH_3), 3.99 (br t, 16 H, $CH_2(CH_2)_4CH_3$), 7.83 (br t, 2 H, Ar*H*), 7.96 (br d, 4 H, Ar*H*), 8.03 (d, J = 7.9 Hz, 4 H, Ar*H*), 8.18 (d, J = 7.9 Hz, 4 H, Ar*H*), 8.25−8.45 (2 × m, 3 H, Ar*H*), 10.21 (s, 4 H, *meso-H*); MS (MALDI, *m*/*z*) 2229 [(M + H)$^+$]; UV/vis (CH_2Cl_2) λ_{max} (log ϵ) 412 (6.22), 538 (4.93), 574 (4.65). HRMS calcd for $C_{147}H_{186}N_8O_2NaZn_2$ 2246.3174, found 2246.3111.

Nickel-5-(4-*tert*-butylphenyl)-10-(4-hydroxymethylphenyl)-2,8,12,18-tetrahexyl-3,7,13,17-tetramethylporphyrin (4). 4 was prepared (0.5−1.0 g scale) as a red powder in 26% overall yield from **10** by mixed aldehyde condensation and metalation according to a previously reported procedure:[8] ^{1}H NMR (400 MHz, $CDCl_3$) δ 1.00 (t, J = 7.2 Hz, 12 H, $(CH_2)_5CH_3$), 1.37−1.57 (2 × m, 16 H, $(CH_2)_3(CH_2)_2CH_3$), 1.62 (s, 9 H, *t-Bu*), 1.71 (apparent quintet, J = 7.3 Hz, 8 H, $(CH_2)_2CH_2(CH_2)_2CH_3$), 2.10 (apparent quintet, J = 7.3 Hz, 8 H, $CH_2CH_2(CH_2)_3CH_3$), 2.30 (s, 6 H, pyrrolic CH_3), 2.32 (s, 6 H, pyrrolic CH_3), 3.73 (t, J = 7.6 Hz, 8 H, $CH_2(CH_2)_4CH_3$), 5.01 (s, 2 H, CH_2OH), 7.65 (d, J = 7.9 Hz, 2 H, Ar*H*), 7.70 (d, J = 8.2 Hz, 2 H, Ar*H*), 7.82 (d, J = 8.1 Hz, 2 H, Ar*H*), 7.89 (d, J = 7.9 Hz, 2 H, Ar*H*), 9.52 (s, 2 H, *meso-H*); ^{13}C NMR (100.6 MHz, $CDCl_3$) δ 10.3, 11.3, 11.6, 19.4, 23.1, 23.2, 26.8, 26.9, 28.9, 29.0, 29.1, 30.1, 32.3, 64.6, 97.5, 118.3, 119.1, 127.1, 128.8, 136.0, 136.6, 141.9, 142.5, 143.0, 143.1, 143.2, 144.2, 144.6, 144.7, 144.8, 147.9, 148.0, 156.0; MS (MALDI, *m*/*z*) 998 (M$^+$); UV/vis (CH_2Cl_2) λ_{max} (log ϵ) 408 (5.20), 528 (4.12), 564 (3.99). HRMS calcd for $C_{65}H_{86}N_4ONaNi$ 1019.6047, found 1019.6041.

Zinc-5-(4-*tert*-butylphenyl)-10-(4-hydroxymethylphenyl)-2,8,12,18-tetrahexyl-3,7,13,17-tetramethylporphyrin (5). Zn porphyrin **5** was prepared (0.5−1.0 g scale) in 32% overall yield from **10** by mixed aldehyde condensation and metalation according to a previously reported procedure:[8] ^{1}H NMR (250 MHz, $CDCl_3$) δ 0.92 (t, J = 7.1 Hz, 12 H, $(CH_2)_5CH_3$), 1.20−1.58 (2 × m, 16 H, $(CH_2)_3(CH_2)_2CH_3$), 1.64 (s, 9 H, *t-Bu*), 1.75 (apparent quintet, J = 7.4 Hz, 8 H, $(CH_2)_2CH_2(CH_2)_2CH_3$), 2.18 (apparent quintet, J = 7.4 Hz, 8 H, $CH_2CH_2(CH_2)_3CH_3$), 2.45 (s, 6 H, pyrrolic CH_3), 2.46 (s, 6 H, pyrrolic CH_3), 3.95 (t, J = 7.3 Hz, 8 H, $CH_2(CH_2)_4CH_3$), 5.06 (d, J = 4.0 Hz, 2 H, CH_2OH), 7.72 (d, J = 7.3 Hz, 2 H, Ar*H*), 7.75 (d, J = 8.2 Hz, 2 H, Ar*H*), 7.97 (d, J = 7.8 Hz, 2 H, Ar*H*), 8.07 (d, J = 8.2 Hz, 2 H, Ar*H*), 10.16 (s, 2 H, *meso-H*); ^{13}C NMR (62.9 MHz, $CDCl_3$) δ 14.1, 15.1, 15.4, 22.7, 26.8, 30.0, 31.8, 32.0, 33.3, 35.0, 65.5, 97.5, 118.8, 119.6, 124.2, 125.9, 132.7, 133.4, 137.9, 138.4, 140.6, 140.8, 143.2, 143.3, 143.4, 146.3, 146.4, 147.6, 148.0, 151.5; MS (MALDI, *m*/*z*) 1004 (M$^+$); UV/vis (CH_2Cl_2) λ_{max} (log ϵ) 410 (5.26), 538 (3.91), 574 (3.65). HRMS calcd for $C_{65}H_{86}N_4ONaZn$ 1025.5985, found 1025.6010.

(Carbonyl)-ruthenium-bis(5,10-(4-hydroxymethylphenyl)-2,8,12,18-tetrahexyl-3,7,13,17-tetramethylporphyrin (16). 16 was prepared, according to the metalation procedure described for **1** and **2** below, in 59% yield from the free-base porphyrin isolated as a side product in the preparation of **5**: ^{1}H NMR (400 MHz, $CDCl_3$ with 5% pyridine-d_5) δ 0.79 (t, J = 7.3 Hz, 12 H, $(CH_2)_5CH_3$), 1.20−1.45 (2 *x* m, 16 H, $(CH_2)_3(CH_2)_2CH_3$), 1.60 (apparent quintet, J = 7.4 Hz, 8 H, $(CH_2)_2CH_2(CH_2)_2CH_3$), 1.95−2.10 (m, 8 H, $CH_2CH_2(CH_2)_3CH_3$), 2.28 (s, 12 H, pyrrolic CH_3), 3.73 (t, J = 7.5 Hz, 8 H, $CH_2(CH_2)_4CH_3$), 5.03 (s, 4 H, CH_2OH), 7.64 (d, J = 7.1 Hz, 2 H, Ar*H*), 7.66 (d, J = 7.1 Hz, 2 H, Ar*H*), 7.88 (d, J = 7.8 Hz, 2 H, Ar*H*), 7.92 (d, J = 7.8 Hz, 2 H, Ar*H*), 9.74 (s, 2 H, *meso-H*); ^{13}C NMR (100.6 MHz, $CDCl_3$ with 5% pyridine-d_5) δ 14.1, 15.4, 22.7, 26.7, 30.0, 31.9, 33.0, 64.9, 98.7, 119.2, 125.4, 125.7, 132.7, 133.3, 137.2, 140.9, 141.2, 143.0; MS (MALDI, *m*/*z*) 1015 [(M + H − CO)$^+$]; UV/vis (CH_2Cl_2) λ_{max} (log ϵ) 402 (5.31), 524 (4.23), 554 (4.12). HRMS calcd for $C_{63}H_{80}N_4O_3Ru$ 1042.4232, found 1043.5393.

Flexible Pentamer 7. A solution of DIAD (160 mg, 0.79 mmol) in 5 mL of THF was added slowly to a solution containing **4** (230 mg, 0.23 mmol), **6** (55 mg, 0.044 mmol), and PPh_3 (320 mg, 1.22 mmol) in THF (30 mL) at room temperature. After stirring the mixture at room temperature for 3 h, the solvent was removed and the residue was purified by SiO_2 chromatography eluting with hexane/ethyl acetate (gradient 10:1 to 5:1) to give **7** as a deep red solid (130 mg, 58%): ^{1}H NMR (250 MHz, $CDCl_3$) δ −2.41 (br s, 2 H, N*H*), 0.70−1.10 (m, 60 H, $(CH_2)_5CH_3$), 1.20−2.50 (4 × m, 168 H, $CH_2(CH_2)_4CH_3$ and CH_2CH_2COO), 1.55 (s, 36 H, *t-Bu*), 2.21 (s, 24 H, pyrrolic CH_3), 2.25 (s, 24 H, pyrrolic CH_3), 2.75 (s, 12 H, core pyrrolic CH_3), 2.81 (t, J = 7.3 Hz, 8 H, CH_2CH_2COO), 3.45−3.75 (m, 32 H, $CH_2(CH_2)_4CH_3$), 3.89 (br t, 8 H, core $CH_2(CH_2)_4CH_3$), 4.30 (t, J = 6.2 Hz, 8 H, $ArOCH_2CH_2$), 5.44 (s, 8 H, $COOCH_2Ar$), 7.05 (br t, 2 H, core Ar*H*), 7.36 (br d, 4 H, core Ar*H*), 7.60 (d, J = 8.2 Hz, 8 H, Ar*H*), 7.64 (d, J = 8.2 Hz, 8 H, Ar*H*), 7.76 (d, J = 7.8 Hz, 8 H, Ar*H*), 7.84 (d, J = 7.8 Hz, 8 H, Ar*H*), 9.40 (s, 8 H, *meso-H*), 10.14 (s, 2 H, *meso-H*);^{13}C NMR (100.6 MHz, $CDCl_3$ with 5% pyridine-d_5) δ 14.1, 14.5, 15.1, 15.4, 22.7, 25.0, 26.3, 26.8, 27.0, 29.3, 29.7, 29.8, 30.0, 31.1, 31.7, 31.9, 32.0, 32.8, 33.3, 34.9, 66.3, 67.3, 96.3, 97.0, 102.1, 112.9, 115.7, 116.7, 117.5, 124.2, 126.9, 128.4, 128.6, 132.6, 133.2, 136.0, 136.1, 138.2, 138.6, 139.2, 139.3, 139.4, 140.2, 140.7, 141.4, 143.4, 143.8, 143.9, 144.1, 144.8, 151.5, 159.5, 173.1; MS (MALDI, *m*/*z*) 5185 [(M + H)$^+$]; UV/vis (CH_2Cl_2) λ_{max} (log ϵ) 408 (5.99), 528 (4.76), 564 (4.86). Anal. Calcd for $C_{336}H_{438}N_{20}O_{12}Ni_4$: C, 77.85; H, 8.52; N, 5.40. Found: C, 77.71; H, 8.56; N, 5.39.

Flexible Pentamer 8. A solution of DIAD (100 mg, 0.50 mmol) in THF (5 mL) was added slowly to a solution containing **5** (120 mg, 0.12 mmol), **6** (30 mg, 0.024 mmol), and PPh_3 (200 mg, 0.76 mmol) in THF (15 mL) at room temperature. After stirring the mixture at room temperature for 3 h, the solvent was removed and the residue was purified by SiO_2 chromatography eluting with hexane/ethyl acetate (gradient 10:1 to 5:1) to give **8** as a purple solid (90 mg, 73%): ^{1}H NMR (400 MHz, $CDCl_3$) δ −2.49 (br s, 2 H, N*H*), 0.70−0.95 (m, 60 H, $(CH_2)_5CH_3$), 1.20−1.48 (2 × m, 80 H, $(CH_2)_3(CH_2)_2CH_3$), 1.60 (s, 36 H, *t-Bu*), 1.60−1.72 (m, 40 H, $(CH_2)_2CH_2(CH_2)_2CH_3$), 2.00−2.20 (2 × m, 48 H, $CH_2CH_2(CH_2)_3CH_3$ and CH_2CH_2COO), 2.28 (s, 24 H, pyrrolic CH_3), 2.36 (s, 24 H, pyrrolic CH_3), 2.60 (t, J = 7.4 Hz, 8 H, CH_2CH_2COO), 2.71 (s, 12 H, core pyrrolic CH_3), 3.70 (t, J = 7.7 Hz, 16 H, $CH_2(CH_2)_4CH_3$), 3.78 (t, J = 7.7 Hz, 16 H, $CH_2(CH_2)_4CH_3$), 3.80−3.90 (m, 8 H, core $CH_2(CH_2)_4CH_3$), 4.21 (t, J = 6.1 Hz, 8 H, $ArOCH_2CH_2$), 5.21 (s, 8 H, $COOCH_2Ar$), 7.05 (t, J = 2.1 Hz, 2 H, core Ar*H*), 7.30 (d, J = 2.1 Hz, 4 H, core Ar*H*), 7.55 (d, J = 7.9 Hz, 8 H, Ar*H*), 7.69 (d, J = 8.3 Hz, 8 H, Ar*H*), 7.89 (d, J = 8.3 Hz, 8 H, Ar*H*), 7.93 (d, J = 7.9 Hz, 8 H, Ar*H*), 9.90 (s, 8 H, *meso-H*), 10.08 (s, 2 H, *meso-H*); ^{13}C NMR (100.6 MHz, $CDCl_3$) δ 14.1, 14.5, 15.0, 15.3, 22.8, 24.8, 26.6, 26.7, 29.8, 30.0, 30.1, 31.0, 31.9, 32.0, 33.3, 35.0, 66.4, 67.3, 96.9, 97.3, 102.0, 113.0, 117.5, 118.3, 119.5, 124.2, 126.9, 128.4, 128.6, 132.8, 133.4, 135.0, 136.1, 137.6, 138.2, 140.6, 141.4, 143.3, 143.4, 144.2, 144.8, 146.1, 146.2, 147.4, 147.9, 151.4, 159.5, 173.1; MS (MALDI, *m*/*z*) 5212 [(M + H)$^+$]; UV/vis (CH_2Cl_2) λ_{max} (log ϵ) 410 (6.20), 540 (4.90), 574 (4.59). Anal. Calcd for $C_{336}H_{438}N_{20}O_{12}Zn_4 \cdot 2H_2O$: C, 76.92; H, 8.49; N, 5.34. Found: C, 76.71; H, 8.12; N, 4.82.

Flexible Pentamer 1. Tris-ruthenium dodecacarbonyl[10] (80 mg, 0.13 mmol) was added to a solution of **7** (125 mg, 0.024 mmol) in toluene (30 mL). The mixture was freeze−pump−thaw degassed once and stirred at reflux for 18 h. The mixture was allowed to cool; the solvent was then removed and the residue purified by SiO_2 chromatography eluting with hexane/ethyl acetate (gradient 10:1 to 5:1) to give **1** as a deep red solid (85 mg, 66%): ^{1}H NMR (250 MHz, $CDCl_3$) δ 0.70−1.10 (m, 60 H, $(CH_2)_5CH_3$), 1.20−1.70 (3 × m, 120 H, $CH_2CH_2(CH_2)_3CH_3$), 1.56 (s, 36 H, *t-Bu*), 1.70−1.90 (m, 8 H, CH_2CH_2COO), 1.90−2.40 (m, 40 H, $CH_2CH_2(CH_2)_3CH_3$), 2.22 (s, 24 H, pyrrolic CH_3), 2.24 (s, 24 H, pyrrolic CH_3), 2.69 (s, 12 H, core pyrrolic CH_3), 2.78 (t, J = 7.5 Hz, 8 H, CH_2CH_2COO), 3.64 (br t, J = 7.2 Hz, 32 H, $CH_2(CH_2)_4CH_3$), 3.91 (br t, 8 H, $CH_2(CH_2)_4CH_3$), 4.20−4.40 (m, 8 H, $ArOCH_2CH_2$), 5.42 (br s, 8 H, $COOCH_2Ar$), 7.03 (br t, 2 H, core Ar*H*), 7.29−7.34 (m, 2 H, core Ar*H*), 7.34−7.40

(m, 2 H, core Ar*H*), 7.59 (d, J = 7.8 Hz, 8 H, Ar*H*), 7.63 (d, J = 8.2 Hz, 8 H, Ar*H*), 7.75 (d, J = 7.8 Hz, 8 H, Ar*H*), 7.84 (d, J = 8.2 Hz, 8 H, Ar*H*), 9.43 (s, 8 H, *meso-H*), 10.03 (s, 2 H, *meso-H*);[13]C NMR (250 MHz, $CDCl_3$) δ 14.2, 15.2, 15.5, 22.8, 25.0, 26.4, 27.0, 29.9, 30.3, 31.1, 31.8, 31.9, 32.0, 32.8, 33.3, 34.9, 66.3, 67.4, 96.4, 99.4, 102.3, 112.9, 113.6, 115.7, 116.7, 119.7, 124.2, 126.9, 132.6, 133.2, 136.0, 136.1, 137.6, 138.2, 138.7, 139.3, 139.4, 139.5, 140.3, 140.7, 141.4, 141.5, 143.5, 143.5, 143.9, 144.0, 145.0, 151.5, 159.3, 159.5, 173.2; MS (MALDI, m/z) 5283 [$(M - CO)^+$]; UV/vis (CH_2Cl_2) λ_{max} (log ϵ) 406 (5.98), 526 (4.83), 562 (4.87). Anal. Calcd for $C_{337}H_{436}N_{20}O_{13}Ni_4Ru\cdot 2H_2O$: C, 75.70; H, 8.29; N, 5.24. Found: C, 75.50; H, 8.06; N, 4.96.

Flexible Pentamer 2. Tris-ruthenium dodecacarbonyl[10] (20 mg, 0.031 mmol) was added to a solution of **8** (40 mg, 0.008 mmol) in toluene (15 mL). The mixture was freeze−pump−thaw degassed once and stirred at 100 °C for 39 h. The mixture was allowed to cool; the solvent was removed and the residue then purified by SiO_2 chromatography eluting with hexane/ethyl acetate (gradient 10:1 to 5:1) to give **2** as a red solid (25 mg, 61%): ^{1}H NMR (250 MHz, $CDCl_3$) δ 0.70−1.00 (m, 60 H, $(CH_2)_5CH_3$), 1.20−1.60 (m, 80 H, $(CH_2)_3(CH_2)_2CH_3$), 1.60−2.40 (3 × m, 88 H, $CH_2(CH_2)_2(CH_2)_2CH_3$ and CH_2CH_2COO), 1.61 (s, 36 H, *t-Bu)*, 2.29 (s, 24 H, pyrrolic CH_3), 2.35 (s, 24 H, pyrrolic CH_3), 2.58 (br t, 8 H, CH_2CH_2COO), 2.68 (s, 12 H, core pyrrolic CH_3), 3.60−4.00 (m, 40 H, $CH_2(CH_2)_4CH_3$), 4.10−4.30 (m, 8 H, $ArOCH_2CH_2$), 5.18 (s, 8 H, $COOCH_2Ar$), 7.04 (br t, 2 H, core Ar*H*), 7.20−7.40 (2 × m, 4 H, core Ar*H*), 7.55 (d, J = 7.9 Hz, 8 H, Ar*H*), 7.70 (d, J = 8.2 Hz, 8 H, Ar*H*), 7.89 (d, J = 7.9 Hz, 8 H, Ar*H*), 7.95 (d, J = 8.2 Hz, 8 H, Ar*H*), 9.90 (br s, 8 H, *meso-H*), 10.00 (s, 2 H, *meso-H*); ^{13} C NMR (100.6 MHz, $CDCl_3$) δ 14.1, 15.0, 15.2, 22.8, 24.8, 26.6, 29.9, 30.1, 30.2, 30.9, 31.8, 32.0, 33.3, 34.9, 66.3, 67.3, 97.3, 99.3, 112.9, 118.3, 119.5, 119.6, 124.2, 126.9, 132.7, 133.3, 135.8, 137.5, 137.6, 138.2, 140.6, 141.4, 141.5, 143.0, 143.3, 143.4, 145.0, 146.1, 146.2, 147.4, 147.9, 151.4, 159.5, 173.1; MS (MALDI, m/z) 5309 [$(M - CO)^+$]; UV/vis (CH_2Cl_2) λ_{max} (log ϵ) 410 (6.27), 540 (5.08), 574 (4.78). Anal. Calcd for $C_{337}H_{436}N_{20}O_{13}Zn_4Ru\cdot 3H_2O$: C, 75.07; H, 8.26; N, 5.20. Found: C, 74.78; H, 8.06; N, 5.09.

Rigid Pentamer 3. A solution of DIAD (85 mg, 0.42 mmol) in THF (5 mL) was added slowly to a solution containing **13** (190 mg, 0.085 mmol), **16** (36 mg, 0.035 mmol), and PPh_3 (200 mg, 0.76 mmol) in THF (25 mL) at 0 °C. After stirring of the mixture at room temperature for 15 h, solvent was removed and the residue was purified by SiO_2 chromatography eluting with hexane/ethyl acetate (10:1) to give **3** as a red solid (40 mg, 21%): ^{1}H NMR (400 MHz, $CDCl_3$) δ 0.80−1.00 (m, 60 H, $(CH_2)_5CH_3$), 1.30−1.60 (2 × m, 80 H, $(CH_2)_3(CH_2)_2CH_3$), 1.51 (s, 72 H, *t-Bu*), 1.65−1.85 (m, 40 H, $(CH_2)_2CH_2(CH_2)_2CH_3$), 2.10−2.30 (m, 40 H, $CH_2CH_2(CH_2)_3CH_3$), 2.44 (s, 24 H, Zn-pyrrolic CH_3), 2.58 (s, 24 H, Zn-pyrrolic CH_3), 2.40−2.60 (br resonances, 12 H, Ru-pyrrolic CH_3), 3.80−4.06 (m, 16 H, $CH_2(CH_2)_4CH_3$), 5.91 (s, 4 H, $ArCH_2O$), 7.81 (t, J = 1.8 Hz, 4 H, Ar*H*), 7.93 (d, J = 1.7 Hz, 8 H, Ar*H*), 7.90−8.30 (br resonances, 8 H, Ar*H*), 8.06 (d, J = 8.1 Hz, 8 H, Ar*H*), 8.19 (d, J = 8.1 Hz, 8 H, Ar*H*), 8.33 (t, J = 1.7 Hz, 2 H, Ar*H*), 8.63 (d, J = 1.7 Hz, 4 H, Ar*H*), 10.01 (s, 2 H, *meso-H*), 10.21 (s, 8 H, *meso-H*); MS (MALDI, m/z) 5432 [$(M - 2H - CO)^+$]; UV/vis (CH_2Cl_2) λ_{max} (log ϵ) 412 (6.11), 540 (4.87), 574 (4.58). Anal. Calcd for $C_{357}H_{448}N_{20}O_5Zn_4Ru\cdot 2H_2O$: C, 77.99; H, 8.29; N, 5.09. Found: C, 77.72; H, 8.23; N, 4.49.

Acknowledgment. We wish to thank The Croucher Foundation, the EPSRC, the University of Cambridge, and the Italian MURST for financial support.

JO001564O